Soft Matter

Dynamic Article Links ►

Cite this: DOI: 10.1039/c0xx00000x

www.rsc.org/softmatter

Paper

Fracture of Metal Coated Elastomers

Nicholas J. Douville,[a] Zhengyu Li[b] Shuichi Takayama[a,c,d], and M.D. Thouless *[b,e]

Received (in XXX, XXX) Xth XXXXXXXXX 20XX, Accepted Xth XXXXXXXXX 20XX
DOI: 10.1039/b000000x

Polydimethyldisiloxane (PDMS) substrates were coated with thin layers of gold varying in thickness between 40 nm and 160 nm. Arrays of parallel cracks formed when a tensile strain was applied to the coated system, with the spacing between the cracks being approximately inversely proportional to the strain. When the crack profiles were examined, it was noted that the cracks extended deep into the substrate – to depths up to two orders of magnitude greater than the film thickness. This extension of the cracks into the substrate is the result of the large mismatch in elastic properties between the metal and soft substrate, and plays a role in the development of the cracking pattern. Despite the relatively large strains that can be applied through the elastomeric substrate, there was no evidence of macroscopic plasticity in the metal films, and numerical analyses showed that the crack profiles were consistent with elastic deformation of the metal. A quantitative comparison of the crack depth and spacing with the predictions of a companion mechanics analysis indicated that the observed spacing and depth were consistent with the metal film being much tougher than the elastomeric substrate. However, for this level of toughness to be exhibited in a metal film would require plastic deformation over a scale much larger than would be expected in such a geometry. This inconsistency may be resolved by recognizing that rupture of a thin metal film can be associated with shear localization that results in a mode-II failure, rather than by classical mode-I crack propagation. This results in a failure mechanism for a metal film that is a high-strain, but low-energy process, with substrate cracking absorbing the excess elastic energy available upon rupture of the film. Such a failure mechanism is consistent with earlier observations for the failure of thin metal films, and this work suggests that failure of an elastomeric substrate may contribute to an additional loss of constraint enhancing this localization.

Introduction

Understanding the mechanics of deformation and failure of a stiff film supported on an elastomeric substrate is important for a number of potential applications. These include the design and fabrication of flexible electronics,[1,2] sensitive skins for machines,[3,4] elastomeric actuators,[5,6] and the use of patterns for fabrication systems.[7,8,9] Under a compressive loading, it is well known that the stiff film deforms by a surface-buckling phenomenon.[10,11,12] Conversely, the film can rupture in response to a tensile strain.[13,14,15,16,17,18,19,20] Two basic mechanisms for the rupture of stiff films on elastomers have been discussed in the literature; one based on instabilities (flow instabilities associated with plastic deformation of a ductile film);[21,22] the other based on fracture of brittle films (with or without accompanying delamination).[6,16,17] The discussions of these models have all been predicated on the assumption that the failure process does not extend into the substrate. In this paper we have identified and characterized a new failure mechanism in which failure of the film is coupled with fracture of the substrate. We have shown that when a metal film on an elastomeric substrate fractures, the cracks can extend into the substrate to depths up to two orders of magnitude greater than the film thickness. In other words, a metal film that is only 100 nm thick can control cracks extending 10 μm into the substrate.

Linear-elastic fracture mechanics can be used to show that a crack can channel across a film supported on a substrate upon the application of a critical tensile strain.[23,24] If the crack remains in the film, the critical strain, ε_c, required to introduce a single crack into a stiff film of thickness h, toughness Γ_f and plane-strain modulus $\overline{E}_f$ on a very thick compliant substrate of modulus $\overline{E}_s$ is approximately given by[24]

$$\varepsilon_c \approx 1.17\left(\frac{\overline{E}_s}{\overline{E}_f}\right)^{0.885}\left(\frac{\Gamma_f}{\overline{E}_s h}\right)^{0.5}, \qquad (1)$$

Above this critical strain, a series of approximately periodic parallel cracks can channel across the film.[26,27,28,29] While details of the spacing between the cracks often depend on stochastic effects,[26] fracture-mechanics analyses indicate that the characteristic spacing between the cracks in these arrays is approximately inversely proportional to the strain and increases with film thickness.[27,28,29] It also increases as the stiffness of the film increases, since the length over which strains build up from a crack surface increases with modulus-mismatch ratio.[30]

When the surface of an elastomer such as polydimethylsiloxane (PDMS) is oxidized, a stiff brittle layer is formed. The periodic channel cracks that can be formed upon the application of a tensile strain have been shown to be useful for various nano- and biological applications.[7,8,31,32,33] However, the ambiguity associated with the parameters of an oxidized surface layer (thickness, modulus, property gradients, and variability of oxidation conditions) prompted an interest in exploring the fracture behavior of a film with relatively well-controlled properties, and a well-defined interface between film and substrate (thickness, modulus, property gradients, and variability of oxidation conditions) prompted an interest in exploring the fracture behavior of a film with relatively well-controlled properties. For this reason, a system consisting of PDMS coated with gold was chosen for study. Gold films are also of practical interest as they have the advantage of providing additional control of the surface chemistry for biomedical applications such

as using self-assembled monolayers (SAMs) for controlled cell adhesion.[34]

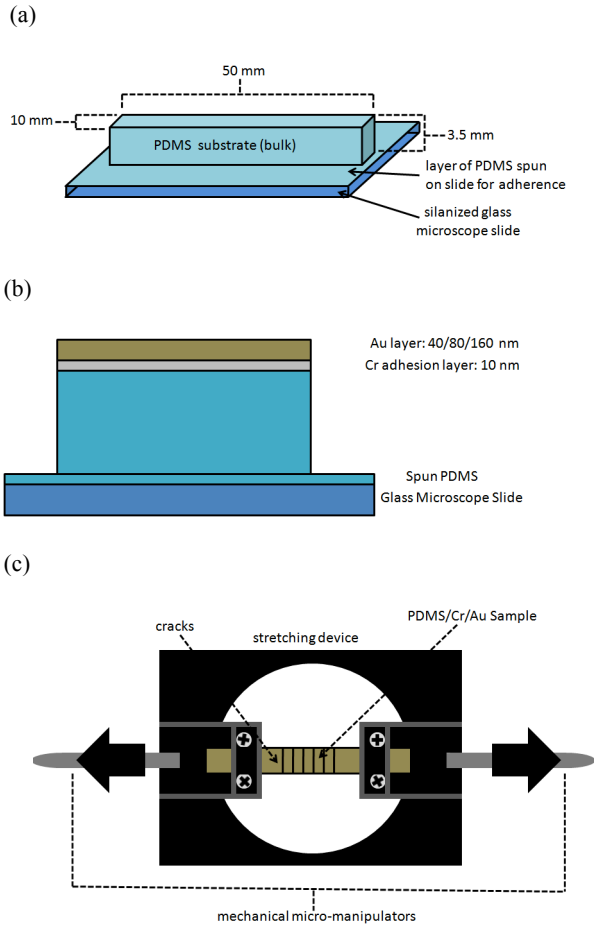

Figure 1 ***(a)*** *PDMS substrate fastened to silanized glass slide with a thin layer of spin-coated PDMS.* ***(b)*** *Coated system with 3.5 mm thick PDMS substrate, 10 nm Cr bonding layer, and 40/80/160 nm thick Au layer.* ***(c)*** *System in mechanical testing device results in a series of cracks upon the application of tensile strain.*

While the modulus mismatch between gold and PDMS is about two orders of magnitude greater than the range studied in many studies of thin-film cracking, the observations in this study were superficially consistent with what would have been expected by extrapolation from the analyses based on fracture mechanics, with crack spacings up to four orders of magnitude greater than the film thickness. However, a more careful examination of the experimental results indicated that the PDMS also fractured as the crack arrays channeled across the gold film. In this paper we give experimental details of this phenomenon, and discuss it in the light of a general fracture-mechanics analysis presented in a companion paper that was originally motivated by the observations described here.[35]

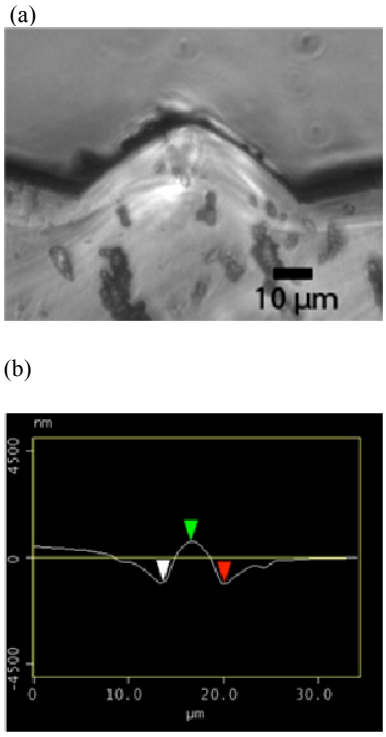

Figure 2 ***(a)*** *Optical micrograph of sectioned replica showing typical profiles of a crack generated at a strain of 25% for a specimen with a 160 nm Au layer. The replica is at the bottom of the image.* ***(b)*** *AFM images of a replica showing a typical profile of a crack generated at a strain of 10% for a specimen with a 40 nm Au layer. In subsequent figures, the crack opening is defined as the distance between the points of maximum rise at the crack mouth, and the crack depth is defined as the distance between these two points and the crack tip. The crack spacing is defined as the distance between neighbouring crack tips in a relaxed state.*

Experimental Methods

An elastomeric substrate was made for these studies using polydimethylsiloxane (PDMS) (Sylgard 184, Dow Corning) mixed at a ratio of 3 parts polymer base to 1 part curing agent by weight. The pre-polymer was poured into a dish to form a slab of thickness 3.5 mm, and cured in an oven at 60 °C for 4 hours. After curing, the slab was cut into strips 50 mm long and 10 mm wide. The strips were placed onto silanized glass slides covered by a thin spin-coated film of PDMS pre-polymer (Fig. 1a). This PDMS pre-polymer was cured at 60 °C for 4 hours (to give a total curing time of 8 hours for the slabs). This step allowed the slabs to be held flat during handling and coating, but permitted relatively easy removal for subsequent testing. The PDMS was then coated by 10 nm of evaporated Cr to function as an adhesion layer; this was followed by evaporation of an Au layer that was either 40, 80 or 160 nm thick (Fig. 1b). The thickness of the two layers was controlled to within 2 nm using an Inficon® XTC/2 film deposition controller, calibrated according to the procedures specified by the manufacturer. In addition, we also verified the calibration process by using a Dektak 6M stylus profiler to measure directly the thickness of a 10 nm Cr/ 80 nmAu bi-layer deposited on a PDMS substrate along an edge formed by shielding from the deposition process. While the results presented in this paper were taken from systems with evaporated films, similar results were obtained with sputtered films, although it was

noted that a higher compressive stress existed with the sputtered films, as demonstrated by the increased tendency of sputtered films to buckle.

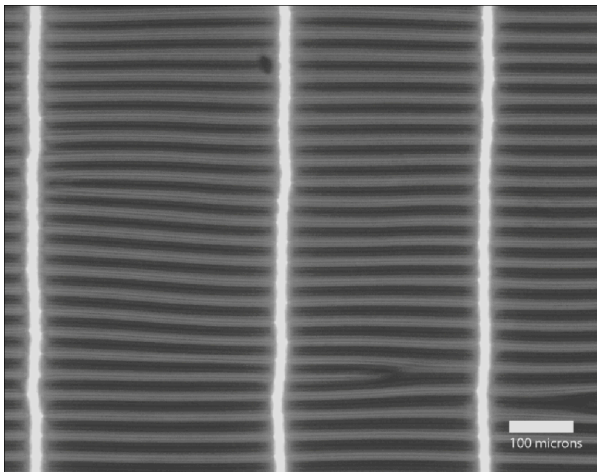

Figure 3. *An example of an optical micrograph showing the formation of periodic cracks in a sample with an 80 nm evaporated Au and 10 nm Cr adhesion layer on PDMS at a nominal strain of 15%. Periodic buckles, induced by Poisson contraction, run perpendicular to the direction of the cracking.*

The modulus and toughness of the PDMS substrate were determined using tension and compact-tension tests,[18] ensuring that the test specimens had undergone the same total curing cycle as the substrates used in the tests. The modulus of the PDMS was found to be 3.8 ± 0.5 MPa. With the assumption of incompressibility for an elastomer, this is equivalent to a plane strain modulus of $\bar{E}_s = 5.1 \pm 0.7$ MPa. The mode-I toughness of the PDMS, Γ_s, was found to be 460 ± 50 J/m^2.

The gold-coated samples were removed from the glass slide using ethanol to wet the interface between the spin-coated PDMS film and glass slide. The samples were then fastened into a mechanical micro-tensile tester mounted in an optical microscope (Fig. 1c) that enabled the system to be stretched at a nominal-strain rate of approximately 0.005 per second. Periodic cracks were observed to channel across the system during these tensile tests. The spacing between neighbouring pairs of cracks was measured as a function of strain using *in-situ* optical microscopy. At pre-determined levels of applied strain, the strain was held fixed and replicas of the surface were made using PDMS prepared by mixing the curing agent and polymer base in a ratio of 1:3 by weight. Prior to replica formation, the surface (thin metal film and exposed PDMS cracks) of the system was silane treated according to a protocol described by Mills *et al*.[18] This silane treatment prevented the PDMS replica from cross-linking with native PDMS and ensured complete removal following polymerization. These replicas were stripped from the cracked surface after being cured at room temperature for 24 hours, and sectioned in a longitudinal direction. Optical microscopy was used to determine the crack profiles from these sections for the 80 and 160 nm thick Au films (Fig. 2a). However, the limitations of optical resolution required the profiles for the 40 nm Au films to be determined by atomic-force microscopy (AFM) of the top surfaces of the replicas (Fig. 2b). The profiles obtained by these techniques were subsequently summarized in terms of a crack opening (distance between the peaks on either side of the crack) and crack depth (distance from peak to trough). The three points used for these definitions are indicated on the AFM trace of Fig. 2b.

Experimental Results

It was noted that there was a small residual compression in the film, as indicated by a periodic array of buckles, before beginning the tensile tests. As the buckles appeared only *after* the PDMS was released from the glass slide, it is believed that this compressive stress was induced by the thermal-expansion mismatch between the PDMS substrate and the glass slide to which it was bonded before the evaporation of the metal film[‡]. For a system with 80 nm Au and 10 nm Cr, the wavelength of these buckles was very regular and equal to about 45 μm. The buckles were aligned perpendicular to the tensile axis of the specimen (the long axis of the specimens - the presence of free surfaces appears to have relaxed the compression in the orthogonal, narrower, direction). Upon the initial application of a tensile strain, these buckles disappeared. However, after the cracks formed, a different set of buckles were formed. These new buckles were parallel to the tensile axis and perpendicular to the cracks (Fig. 3), as has been observed in earlier studies for oxidized PDMS.[18] It is believed that these buckles formed from an induced compressive stress arising from the interaction between the Poisson contraction of the substrate below the cracks and the relaxation of the applied strain in the region between the cracks. The average wavelength for these buckles was about 32 μm. A difference in wavelengths between the buckles associated with a relaxed tension and the buckles associated with cracking was a very consistent feature of these studies, and earlier studies on oxidized PDMS.[36] Furthermore, both sets of wavelengths were much larger than that which is predicted by standard results for buckling on a compliant substrate, in which the wavelength, λ, is related to the film thickness, h, by:[37]

$$\lambda = 2\pi h\left(\bar{E}_f / 3\bar{E}_s\right)^{1/3} \quad , \qquad (2)$$

which would indicate a wavelength of about 9 μm for a gold film of 80 nm (compared to the experimentally observed wavelength of approximately 45 μm for the uncracked system). Even recognizing that the experimental configuration is a bi-layer, this discrepancy is outside the range of what can reasonably be explained by experimental uncertainty, precluding the use of these buckling equations in further analysis, such as estimation of residual compression.[‡‡]

Figure 4 shows a plot of the average crack spacing as a function of applied nominal strain. The average spacing at a given strain ε_o was determined from the average of *in-situ* optical measurements of the distance between individual pairs of neighbouring cracks, and corrected by a factor $1/(1+\varepsilon_o)$ to compensate for the stretching. The error bars represent one standard deviation in the crack spacing from multiple pairs of cracks. At high strains, each datum point in the figure corresponds to an average from up to 100 crack pairs. Cracks were observed down to nominal strains of just below 1%.

[‡] *An initial compressive strain of about 0.5% in the metal film was estimated from the quoted values for the coefficient of thermal expansion for PDMS and glass, and the curing temperature of 60 ºC.*

[‡‡] *A similar discrepancy has been reported elsewhere for an Au/PDMS system.[12] In this earlier report, it was suggested that a possible origin for the discrepancy was a high temperature during the evaporation process forming a surface layer. However, in the present case, the temperatures during evaporation were measured with thermocouples; they never exceeded the curing temperature of the PDMS.*

However, at these lower strains, the number of cracks in the gauge length was so low that the use of distances between neighbouring cracks to determine the average crack spacing had a statistical effect of slightly under-estimating the average spacing that would be observed in a longer specimen. There was also some ambiguity in these very low strain ranges as to whether any cracks had been introduced by handling prior to straining. Data sets corresponding to less than five observed cracks have not been included in Fig. 4.

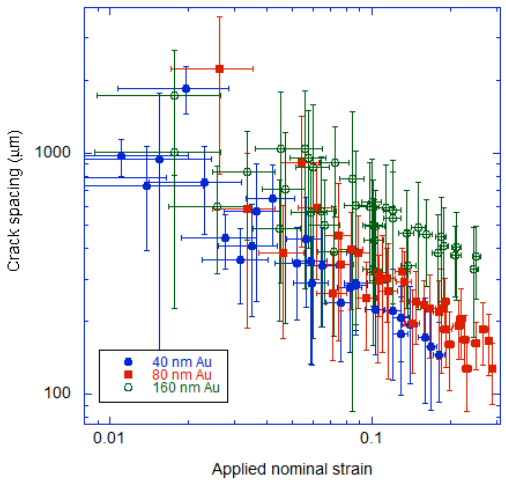

Figure 4. *Average crack spacing as function of applied nominal strain. The error bars represent one standard deviation in the crack spacing.*

Fig. 5 shows a plot of the average crack depth as a function of nominal strain. These values were determined from between 10 and 20 crack profiles obtained from replicas taken at each strain, as described in the previous section. Of particular significance is that the depth of the cracks is in the range of 5 to 15 µm, compared to a total film thickness of between 50 nm and 170 nm. Since the replicas were taken under strained conditions (so the cracks were relatively open) the crack profiles were probably fairly faithfully replicated. Direct images of the cracks were obtained using a 3D measuring laser microscope (Olympus OLS4000) at 50x magnification to validate that these crack profiles were not artifacts of the replica process.

While an average crack spacing could be determined for a given strain, the stochastic nature of the cracking process meant that the cracks were not uniformly spaced across the film. Furthermore, there was no uniformity in the depth and opening of the cracks. This is illustrated by the data plotted in Fig. 6. The profiles of a series of cracks were measured from the replicas along with the distance to the nearest neighbouring cracks on both sides. The depth and opening of the cracks is plotted in Fig. 6 as a function of this average spacing, with the width of the error bars indicating the distance to the nearest crack (so a small error bar in this figure corresponds to a more symmetrical crack). It should be noticed that openings of many tens of microns are consistent with the fact that the cracks are clearly visible by low powered optical microscopy (Fig. 3), and is consistent with the very deep cracks. Had the cracks remained within the metal layer, with the layer bonded to the substrate, the crack openings would have been much smaller than actually observed.

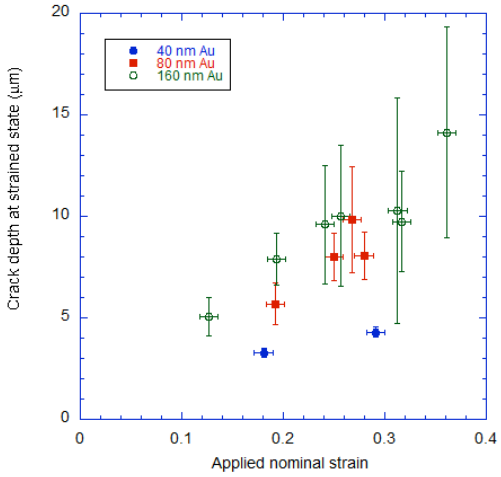

Figure 5. *Average crack depth as function of applied nominal strain. The uncertainties represent one standard deviation of depths from all. The crack depth is an underestimate, because it has not been corrected for the applied strain (which makes the cracks wider and shallower).*

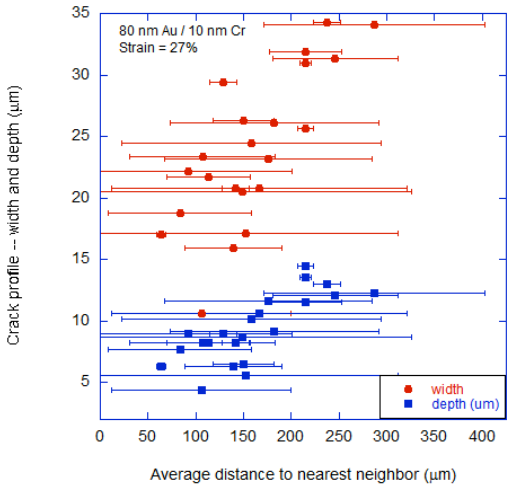

Figure 6. *Dependence of the crack opening and crack depths on the average distance to the nearest neighbour for one particular value of applied nominal strain. The range of the uncertainties for the spacing in this plot represents the maximum and minimum distances to the nearest crack. A small uncertainty indicates a crack more nearly in the middle of two neighbours.*

Discussion

The most striking aspect of the experimental results was the relatively great depth to which the cracks propagated within the

substrate. This was apparent from the replica studies and from the optical observations of the crack opening. As discussed below, finite-element calculations showed that the profile of the crack surface could only be explained by these deep cracks. Furthermore, it should be noted that it is actually a well-known mechanics result that a crack within a stiff layer should be drawn across an interface into a more compliant material.[24,38] However, despite the fact that, in retrospect, crack propagation in an elastomeric substrate might be expected, this phenomenon has not been previously noted or analyzed. Prompted by the observations described in this paper, a general linear-elastic fracture-mechanics analysis of cracking in stiff films on compliant substrates was developed and has been presented elsewhere.[35] Here, the experimental results presented above are discussed in the light of the insight provided by this general analysis.

Strain level in the metal film

The nominal strains applied to the substrate are sufficiently large, being in excess of 20%, that there is an immediate question about the validity of a linear-elastic analysis. As detailed elsewhere[18] and verified again for this study, the PDMS itself behaves in a linear fashion at nominal strains up to about 40%. The cracks, and the depth to which they propagate, reduce the strain in the film to a level well below the nominal strain applied to the substrate. The extent of this reduction can be deduced by a finite-element calculation that accurately includes the crack spacing, depth, and elastic properties. The PDMS was modelled with a modulus of 3.8 MPa and an assumed Poisson's ratio of 0.4995 using hyper-elastic elements in the commercial finite-element program ABAQUS. The metal films were modelled using incompatible-mode elements. The modulus and Poisson's ratio of Cr were assumed to be 279 GPa and 0.21; the elastic properties of Au were assumed to be 78 GPa and 0.44.[38] Initially, the films were assumed to deform only in an elastic fashion.

Owing to the huge modulus mismatch between the PDMS and metallic layer, the full depth of 3.5 mm for the substrate was modelled (along with the correct thickness of the Cr and Au layers). A segment of the system containing a set of cracks that had been observed experimentally was modelled. While periodic boundary conditions were used at either end of this segment, the crack spacing within the segment were set according to the experimental observations. The mesh was reduced to 10 nm around the crack tips within the PDMS, and a mesh-sensitivity analysis was conducted to assure that any uncertainties from the numerical procedure was less than the uncertainties from the experimental observations. The calculations were done for a number of different sets of data that formed the plot given in Fig. 6 to verify consistency between the results, but one particular set will serve for illustrative purposes. Table 1 lists experimental details of a set of five contiguous cracks, with the measured spacing, depth and opening at a nominal strain of 25%. The periodic boundary conditions were imposed on the plane at the centre of the first and last cracks of the series, and the appropriate level of strain was introduced by the imposition of a uniform displacement between these boundaries under plane-strain conditions.

Figure 7 shows the deformed mesh that results from the crack distribution given in Table 1. While the crack depths and spacings were chosen *a priori* to match the experimental measurements, the crack openings were left as parameters to be determined as outputs from the numerical calculations. A subsequent comparison with the experimental observations (Table 1) shows that these completely elastic calculations describe the openings very well. The fact that the crack profiles predicted from an elastic calculation matched the experimental observations so well, indicates that the metal film does not deform plastically to any significant extent. (Plastic deformation of the film would have reduced the crack opening). The calculations indicated that the strain in the film increased with distance from the cracks, and reached a maximum of between about 0.4% and 0.6% halfway between neighbouring cracks. This maximum level of strain was obtained in a reproducible fashion from several related calculations with different experimental data sets, and was therefore taken to be an approximate measure of the strain required to rupture the film.

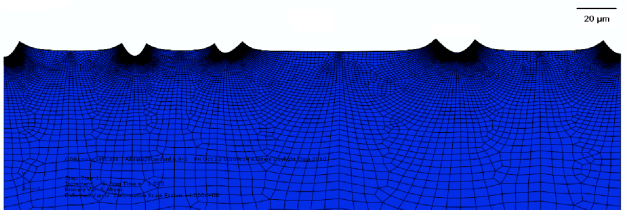

Figure 7. *Output from a finite-element calculation for a system with 10 nm of Cr, 80 nm of Au and a nominal strain of 25%, with crack depths and spacing set by experimental observations. The peaks to either side of the cracks (which match the experimental profiles as shown in Fig. 2) are the result of a Poisson's ratio effect. The stress is relaxed near the crack surfaces, causing the out-of-plane displacement to be relaxed.*

		Observed (± 1 μm)	Calculated
crack 1	opening (μm) depth (μm)	19 8	16 8
space (μm) maximum computed strain		68	70 0.45%±0.05%
crack 2	opening (μm) depth (μm)	15 7	13 7
space (μm) maximum computed strain		46	49 0.41%±0.05%
crack 3	opening (μm) depth (μm)	14 6	15 5-6
space (μm) maximum computed strain		129	123 0.60%±0.05%
crack 4	opening (μm) depth (μm)	17 7	21 7
space (μm) maximum computed strain		86	88 0.50%±0.05%
crack 5	opening (μm) depth (μm)	18 7	18 7

Table 1. *A comparison between observed crack data and the finite-element calculation shown in Fig. 7 that was used to estimate the strain level in the metal film (nominal strain applied to the system = 25%,;10 nm Cr and 80 nm Au)*

Comparison of observations with related elastic fracture-mechanics analysis

A major conclusion of the finite-element calculations described above is that the metal film deforms elastically up to strains of about 0.6% before fracture occurs. This level of elastic strain, indicating a yield stress of 475 MPa or more, is consistent with

what might be expected for gold films of this thickness.[40] Furthermore, elastic deformation of the metal film indicates that the problem should be amenable to a linear-elastic fracture mechanics (LEFM) analyses, which allows one to invoke the concept of a fracture toughness for the thin metal film and substrate, as described in the companion analysis.[35]

The LEFM analysis of Ref. [35] is a general one appropriate for a single film of modulus $\bar{E}_f$, toughness Γ_f, and thickness h on a compliant substrate of modulus $\bar{E}_s$, toughness Γ_s, subjected to a nominal applied tensile strain of ε_o. This analysis indicates that cracking of the substrate enhances failure of the system in that it *reduces* the critical strain for propagating a channel crack to below that given by Eqn. 1. Furthermore, above this critical strain, the crack spacing, S, is predicted to be approximately inversely proportional to the applied strain:

$$\frac{S}{h} \propto \frac{1}{\varepsilon_o}\left(\frac{\Gamma_s}{\bar{E}_s h}\right)^{1/2} . \qquad (3)$$

In this relationship, the constant of proportionality is a function of the ratio of Γ_f / Γ_s, with the normalized crack spacing increasing as the toughness ratio increases.[35] As can be seen in the non-dimensional plot of Fig. 8, the experimental data is quite well described by the functional form of Eqn. 3, despite the fact that the experiments involved a bilayer consisting of two different metals. It is noted that the use of a slightly more compliant substrate with a 10:1 ratio of polymer:curing agent resulted in a slightly larger crack spacing for a given nominal strain. This is consistent with Eqn. 3.

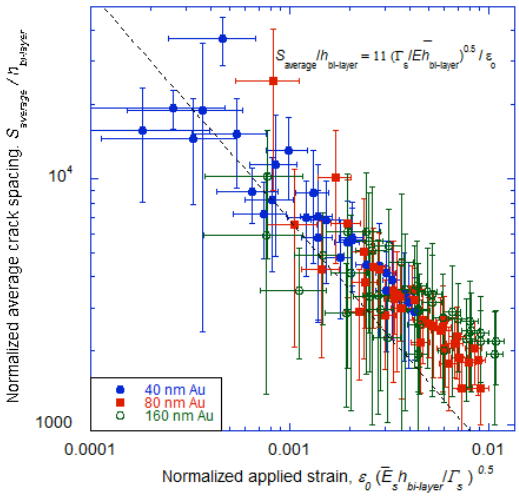

Figure 8. *The experimental data of Fig. 4 replotted in non-dimensional form, to make a comparison with the LEFM analysis.*[35]

The LEFM results indicate that the crack spacing is dependent on both the modulus mismatch and the toughness ratio between the film and substrate.[35] Specific examples of the general results from the mechanics calculation are given in Fig. 9, which shows how the predicted crack spacing varies with applied strain for different levels of toughness ratio between film and substrate. The calculations of Fig. 9 were computed for a modulus-mismatch ratio of $2\text{x}10^4$, which is a good approximation for the mismatch between Au and PDMS. It will be observed that the crack spacing increases for a given level of strain as the toughness ratio film increases. The depth of the crack has also been shown to increase with this ratio.[35]

Superimposed on Fig. 9 is the approximate range for the experimental data for the Au/Cr bi-layers on PDMS. It will be see that the LEFM models provides a reasonable agreement with the experimental results for the crack spacing if the toughness of the metal film is taken to be about 10-50 times greater than that of the substrate. While this toughness of about 4.5-22 kJ/m^2 (corresponding to a fracture toughness, K_{Ic} of about 21-46 MPa$\sqrt{\text{m}}$) is reasonable for bulk metal specimens, it is considerably in excess of what might be expected for a thin film because it would require a plastic zone size much larger than the film thickness. An approximate estimate for the toughness of a thin film is given by the product of the thickness and yield strength.[41] Such a calculation would indicate a toughness of no more than about 50 J/m^2 for a Au film of 80 nm. This is only about 10% of the toughness of the PDMS. Such a low value of toughness would correspond to a very "brittle" film, and the cracks would be expected to penetrate only a little distance into the substrate. Furthermore, the predicted spacing would be considerably more than an order of magnitude less than observed, and the onset of cracking would occur at a relatively low strain.

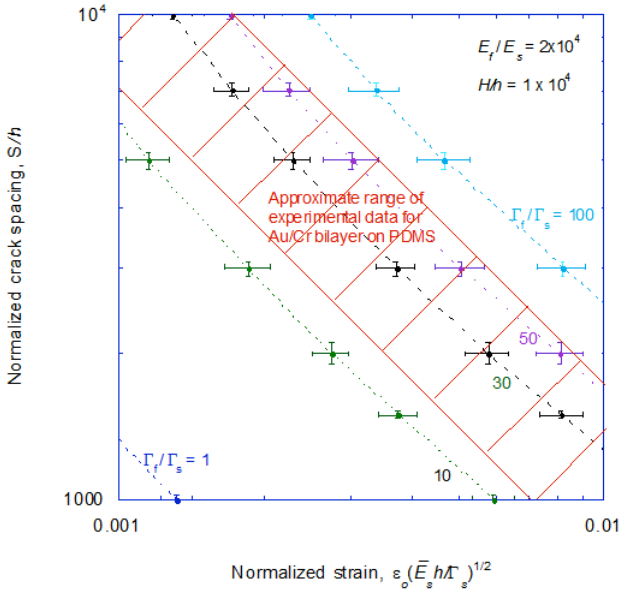

Figure 9. *The results of the LEFM analysis of Ref. [35] calculated for a bilayer, with a modulus mismatch ratio between the film and substrate comparable to the value appropriate for Au on PDMS. Results for different values of the ratio of the film toughness to the substrate toughness, Γ_f / Γ_s, are presented. A comparison to the range of experimental results, indicates that they match the LEFM model for a toughness ratio in the range of 10 to 50.*

The apparent paradox where a thin metal film on a soft substrate that should behave in a relatively brittle fashion, but actually exhibits cracking behaviour consistent with a much tougher material, may perhaps be resolved by recognizing that there is evidence thin gold films do not rupture by a classical mode-I fracture mechanism. In 1960, Pashley performed *in-situ* tensile tests of thin gold films in a transmission electron

microscope.[40] These experiments revealed that free-standing thin gold films deform elastically until failing at relatively high strains by rupture associated with shear localization. For thin films, this rupture mechanism dissipates much less energy than a mode-I fracture mechanism. It is probably related to the well-known fracture-mechanics phenomenon that, while the toughness of metals increases from plane-strain values to plane-stress values as the thickness decreases, the fracture mechanism changes to a shear mode and the toughness drops with sample thickness below a critical thickness.[42] Furthermore, it has been shown for metal films on polymeric substrates that while this shear localization can be suppressed if the substrate is reasonably stiff,[21] the constraint may not be sufficient to suppress the localization if the substrate is an elastomer such as PDMS.[22] The results presented in the present work are consistent with these results from the literature. Furthermore, we have shown that there may be an additional loss of constraint suppressing this localization mechanism associated with fracture of the substrate.

Conclusions

When metal films supported on a very compliant substrate such as PDMS rupture, they can induce fracture of the underlying substrate, with the cracks growing to significant depths below into the substrate. It has been shown in an accompanying paper that this reduces the critical strain at which crack propagation can occur.[35] Despite the large nominal strains that can be imposed on the Au/PDMS system, the strain in the metal film may remain in the elastic regime. This is both because thin films tend to have relatively high yield strengths, and because cracking limits the strain transfer from the substrate to the film. While elastic deformation of the film and substrate implies that the techniques of fracture mechanics may be a valid means to analysis the fracture, the results reinforce the notion that the concept of toughness for such a thin metal layer is ambiguous. The observed strains required for fracture and the corresponding crack spacing seem to be consistent with toughness much higher than is appropriate for an elastic thin film. Rupture of the metal appears to be controlled not by the toughness of the film, but by a critical stress or strain level in the film. Once the film has ruptured, then the cracks can propagate into the substrate. This view of the process is consistent with existing results in the literature that metal films fail by shear localization, and that while a stiff polymer may provide a constraint to suppress this mode of failure, a soft polymer such as PDMS does not provide a sufficient constraint. Fracture of the substrate further reduces any constraint on this failure mode.

Acknowledgments

The authors gratefully acknowledge support from the National Science Foundation (CMMI-0700232) and the National Institute of Health (R01-HG004653-01). NJD was supported by The NHLBI Ruth L. Kirschstein NRSA for Individual Predoctoral MD/PhD Fellows (F30HL095333), as well as, the University of Michigan Medical Scientist Training Program (NIGMS T32 GM07863). We thank Dr. Brian N. Johnson for help with the evaporation of thin metal films in the Chemical Engineering Clean Room at the University of Michigan and Dr. Pilar Herrera-Fierro for assistance with imaging within the Lurie Nanofabrication Facility at the University of Michigan.

Notes and references

[a] *Department of Biomedical Engineering, University of Michigan, 2200 Bonisteel Blvd., Ann Arbor, MI, 48109, USA. Fax: +1-734-936-1905; Tel: +1-734- 615-5539; E-mail: ndouvill@umich.edu, takayama@umich.edu*

[b] *Department of Mechanical Engineering, University of Michigan, 2282 G.G. Brown Building, Ann Arbor, MI 48109, USA. Fax: +1-734- 647-3170; Tel: +1-734-763-2125, E-mail: zhengyul@umich.edu, thouless@umich.edu*

[c] *Macromolecular Science and Engineering Center, University of Michigan, 2300 Hayward St, Ann Arbor, MI, 48109, USA*

[d] *Division of Nano-Bio and Chemical Engineering WCU Project, UNIST, Ulsan, Republic of Korea*

[e] *Materials Science & Engineering, University of Michigan, 3062 H.H. Dow, 2300 Hayward St, Ann Arbor, MI 48109, USA.*

1. J. Lewis, *Mater. Today,* 2004, **9**, 38-45.
2. N.J. Douville, Y.-C. Tung, R. Li, J.D. Wang, M.E.H. El-Sayed, and S. Takayama, *Anal. Chem*., 2010, **82**, 2505-2511.
3. V. J. Lumelsky, M. S. Shur and S. Wagner, *IEEE Sens. J.*, 2001, **1**, 41-51.
4. S.P. Lacour, J. Jones, Z. Suo, and S. Wagner, *IEEE Electr. Devic L.*, 2004, **2**, 179-181.
5. R. Pelrine, R.D. Kornbluh, J. Joseph, R. Heydt, Q. Pei, and S. Chiba. *Materials Science and Engineering C*, 2000, **11**, 89-100.
6. M.R. Begley, H. Bart-Smith, O. N. Scott, M. H. Jones and M. L. Reed, *J. Mech. Phys. Solids*, 2005, **53**, 2557-2578.
7. X. Zhu, K.L. Mills, P.R. Peters, J.H. Bahng, E.H. Liu, J. Shim, K. Naruse, M.E. Csete, M.D. Thouless, and S. Takayama, *Nat. Mater.*, 2005, **4**, 403-405.
8. K. L. Mills, Dongeun Huh, Shuichi Takayama, and M. D. Thouless, *Lab Chip,* 2010, **10**, 1627-1630.
9. S. Chung, J. H. Lee, M. W. Moon, J. Han and R. D. Kamm, *Adv. Mater.*, 2008, **20**, 3011-3016.
10. M. W. Moon, S. H. Lee, J.Y. Sun, K. H. Oh, A. Vaziri and J. W. Hutchinson, *P. Natl. Acad. Sci. USA*, 2007, **104**, 1130-1133.
11. N. Bowden, S. Brittain, A. G. Evans, J. W. Hutchinson and G. M. Whitesides, *Nature*, 1998, **393**, 146-149.
12. X. Chen and J. W. Hutchinson, *J. Appl. Mech.,* 2004, **71**, 597-603.
13. S.P. Lacour, S. Wagner, Z. Huang and Z. Suo, *Appl. Phys. Lett.,* 2003, **82**, 2404-2406.
14. T. Li, Z. Huang, Z. Suo, S.P. Lacour and S. Wagner, *Appl Phys. Lett.,* 2004, **85** 3435-3437.
15. M. R. Begley and H. Bart-Smith, *Int. J. Solids Struct.,* 2005, **42**, 5259-5273.
16. N. E. Jansson, Y. Leterrier and J.-A. E. Månson, *Eng. Fract. Mech.*, 2006, **73**, 2614-2626.
17. D. Tsubone, T. Hasebe, A. Kamijo and A. Hotta, *Surf. Coat. Tech.,* 2007, 6423-6430.
18. K. L. Mills, X. Zhu, S. Takayama and M. D. Thouless, *J. Mater. Res.*, 2008, **23**, 37-48.
19. O. Akogwu, D. Kwabi, S. Midturi, M. Eleruja, B. Babatope and W. O. Soboyejo, *Mat. Sci. Eng. B*, 2010, **170**, 32-40.

20. M.J. Cordill, A. Taylor, J. Schalko and G. Dehm, *Metall. Mater. Trans. A,* 2010, **41A**, 870-874.

21. T. Li, Z.Y. Huang, Z.C. Xi, S.P. Lacour, S. Wagner, and Z. Suo. *Mech. Mater.*, 2005 **37**, 261-273.

22. T. Li and Z. Suo, *Int. J. Solids Struct.,* 2006, **43**, 2351-2363.

23. M. S. Hu, M. D. Thouless and A. G. Evans, *Acta Metall.*, 1988, **36**, 1301-1307.

24. J. L. Beuth Jr., *Int. J. Solids Struct.*, 1992, 2**9**,1657--1675.

25. J. Dundurs, *J. Appl. Mech.*, 1969, **36**, 650-652.

26. M. D. Thouless, *Annu. Rev. Mater. Sci.*, 1995, **25,** 69-96.

27. M. D. Thouless, *J. Am. Ceram. Soc.*, 1990, **73**, 2144-2146 .

28. M. D. Thouless, E. Olsson and A. Gupta, *Acta Metall. Mater.,*1992, **40**, 1287-1292.

29. J. W. Hutchinson and Z. Suo, *Adv. Appl. Mech.*, 1992, **29**, 63-191.

30. V. B. Shenoy, A. F. Schwartzman and L. B. Freund, *Int. J. Fracture*, 2000, **103**, 1-17.

31. D. Huh, K.L. Mills, X. Zhu, M.A. Burns, M.D. Thouless, and S. Takayama, *Nat. Mater*., 2007, **6**, 424-428.

32. H.-N. Kim, S.-H Lee, and K.-Y. Suh*, Lab Chip*, 2011, **11**, 717-722.

33. C. J. Rand, R. Sweeney, M. Morrissey, L. Hazel, and A. J. Crosby, *Soft Matter*, 2008, **4**, 1805-1807.

34. M. Mrksich, C.S. Chen, Y. Xia, L.E. Dike, D.E. Ingber, and G.M. Whitesides, *Proc. Natl. Acad. Sci. USA*, 1996, **96**, 10775-10778.

35. M. D. Thouless, Z. Li, N. J. Douville and S. Takayama, *J. Mech. Phys. Solids*, 2011 (in press, doi:10.1016/j.jmps.2011.04.009)

36. D. Lee, PhD Thesis, University of Michigan (2008).

37. H. G. Allen, *Analysis and Design of Structural Sandwich Panels*, 1969, Pergamon, New York.

38. A. K. Zak and M. L. Williams, *J. Appl. Mech.* 1963, **30**, 142-143.

39. W. F. Smith and J. Hashemi, *Foundations of Materials Science and Engineering*, 2006, New York, NY 10020: The McGraw-Hill Companies, Inc. ISBN: 0072953586

40. D. W. Pashley, *P. R. Soc. London,* 1960, **A255**, 218-231.

41. J.W. Hutchinson, *private communication*, July 2010.

42. D. Broek, *Elementary Engineering Fracture Mechanics,* 3rd. Edition, 1982, Martinus Nijhoff Publishers , The Hague, The Netherlands.